**Journal of Low Temperature Physics manuscript No.**
(will be inserted by the editor)

**John E. Sadleir, Sang-Jun Lee, Stephen J. Smith, Sarah E. Busch, Simon R. Bandler, Joseph S. Adams, Megan E. Eckart, James A. Chevenak, Richard L. Kelley, Caroline A. Kilbourne, Frederick S. Porter, Jan-Patrick Porst**

# The Magnetically-Tuned Transition-Edge Sensor

XX.XX.20XX

**Abstract** We present the first measurements on the proposed magnetically-tuned superconducting transition-edge sensor (MTES) and compare the modified resistive transition with the theoretical prediction. A TES's resistive transition is customarily characterized in terms of the unit less device parameters $\alpha$ and $\beta$ corresponding to the resistive response to changes in temperature and current respectively. We present a new relationship between measured IV quantities and the parameters $\alpha$ and $\beta$ and use these relations to confirm we have stably biased a TES with negative $\beta$ parameter with magnetic tuning. Motivated by access to this new unexplored parameter space, we investigate the conditions for bias stability of a TES taking into account both self and externally applied magnetic fields.

**Keywords** Low Temperature Detectors, Supeconductivity, Magnetic Field dependence, superconducting resistive transition width, superconducting weak-links

## 1 Introduction

Significant progress has been made in transition-edge sensors (TESs) treating the resistive transition $R(T,I)$ as a function of temperature $T$ and current $I$. Recent developments have shown that it is important to also consider the magnetic field dependence $B$ of the resistive transition $R(T,I,B)$.[3] Work extending the TES model to include the magnetic field dependence also found a way to alter the effective width of the resistive transition $\Delta T$, in what the authors called a magnetically-tuned TES or MTES.[1] With magnetic tuning we explained that it is possible to

NASA Goddard Space Flight Center
Greenbelt, MD 20771, USA
Tel.: 301-286-3078
Fax:
E-mail: john.e.sadleir@nasa.gov

reduce $\beta$ while maintaining a large $\alpha$ that will increase the signal size, speed up the pulse recovery time, reduce the performance limiting Johnson noise, and increase the energy resolving power provided no new sources of noise appear. One of the more extreme predictions was that it was possible to not only reduce $\beta$ to values approaching zero but it was also possible to stably bias a MTES with negative $\beta$. In this work we show measurements on a prototype MTES that confirms the predicted change in transition shape with magnetic tuning and also realizes stable bias with a negative $\beta$. To demonstrate stable bias with negative $\beta$ this we derive a new relationship between measured IV quantities. Lastly, we reinvestigate the bias stability conditions for a TES including the magnetic field dependence $B$ of the $R(T,I,B)$.The results are used to show the allowable $\beta$ range with stable solutions and the constraints placed on the other device parameters.

## 2 $R(T,I,B)$ transition

For small signals the TES's $R(T,I,B)$ can be expanded around a point in resistance, temperature, current, and magnetic field space $\mathbf{v_0} = (R_0, T_0, I_0, B_0)$ to first order as

$$R(T,I,B) \approx R_0 + \frac{\partial R}{\partial T}\delta T + \frac{\partial R}{\partial I}\delta I + \frac{\partial R}{\partial B}\delta B, \tag{1}$$

with $\delta T = T - T_0$ , $\delta I = I - I_0$ , $\delta B = B - B_0$ representing the departures away from the initial operating point and all partial derivatives evaluated at $\mathbf{v_0}$.

We define the following parameters as the logarithmic derivative of the resistance with respect to temperature, current, and magnetic field ($\alpha \equiv \frac{T_0}{R_0}\frac{\partial R}{\partial T}$ , $\beta_I \equiv \frac{I_0}{R_0}\frac{\partial R}{\partial I}$ , $\gamma \equiv \frac{B_0}{R_0}\frac{\partial R}{\partial B}$),

where again the partial derivatives are evaluated at the initial operating point in the transition $\mathbf{v_0}$.

Using our $I_c$ rectification model for asymmetric current injection[4] we know we can write the total magnetic field at the TES as $B = B_a + gI$ where $B_a$ is an externally applied magnetic field and $g$ is a geometry-dependent self-fielding factor and $I$ is the TES current. For a constant $B_a$ we have $\delta B = g\,\delta I$.

After substituting the above definitions our Taylor expansion becomes, with $\beta = \beta_I + \beta_B = \beta_I + \frac{gI_0}{R_0}\frac{\partial R}{\partial B}$,

$$R(T,I,B) \approx R_0 + \alpha\frac{R_0}{T_0}\delta T + \beta\frac{R_0}{I_0}\delta I. \tag{2}$$

It was shown that $\beta_I$ is positive and $\beta_B$ can be: positive, go to zero, or negative (corresponding to required conditions for case 0, 1, and 2 respectively in reference[1]). Additionally, $\beta_B$ can be made sufficiently negative such that the overall $\beta$ becomes negative.

## 3 $\alpha_{IV}$ Derivation

In this section we derive a relationship between $\alpha_{IV} \equiv \frac{T}{R}\frac{dR}{dT}$ and the perviously defined parameters $\alpha$ and $\beta$. This relationship is useful as $\alpha_{IV}$ (which is composed

of both $\alpha$ and $\beta$) is obtainable from current $I$ versus voltage $V$ measurements routinely used to determine the thermal conductance to the heat path $G$ and associated thermal power exponent $n$. In contrast, impedance measurements $Z(f)$ are routinely used to find $\alpha$ and $\beta$ by fitting the $Z(f)$ data over a range of bias voltages and frequencies $f$. The $\alpha_{IV}$ relationship also has utility if used as another constraint equation for the $Z(f)$ fits. Lastly, it gives a measure of the important device parameter ratio $\frac{\alpha}{\beta}$ from IV measurements alone in certain limits of operation discussed below.

If we equate the Joule power heating from the biased TES to the heat flow from the TES at temperature $T$ to the heat bath at temperature $T_{bath} \equiv T_b$ we have a thermal equation for the electrical resistance $R_{th}$ satisfying $R_{th} = P_{bath}/I^2$.

After a first order Taylor expansion of $R_{th}(T,I)$, equating to $R(T,I,B)$, and collecting terms we find

$$\alpha_{IV} = \left( I_0 \frac{\partial R_{th}}{\partial I} \alpha - T_0 \beta \frac{\partial R_{th}}{\partial T} \right) \Bigg/ \left( \frac{\partial R_{th}}{\partial I} I_0 - R_0 \beta \right). \tag{3}$$

The equation does not depend upon the specific resistance mechanism or functional form for the TES resistance nor does it depend on the specific functional form describing $P_{bath}$.

If we now assume a specific thermal equation describing the flow of heat to the bath of the form

$$P_{bath} = \frac{G}{nT^{n-1}} \left( T^n - T_b^n \right) = \frac{GT\phi}{n} \tag{4}$$

then we have $R_{th} = \frac{G}{I^2 n T^{n-1}} \left( T^n - T_b^n \right) = \frac{GT\phi}{nI^2}$ with the definition $\phi \equiv 1 - (T_b/T)^n$. The above functional form for $P_{bath}$ gives,

$$\alpha_{IV} = \frac{2\alpha + \beta \left( 1 + n \left( \frac{1}{\phi} - 1 \right) \right)}{2 + \beta}. \tag{5}$$

In the limit $T_b \ll T$, $\phi \to 1$, and $\alpha_{IV} \to \frac{2\alpha+\beta}{2+\beta}$. If we also have $\beta$ large then $\alpha_{IV} \to 1 + 2\frac{\alpha}{\beta}$. From the definition of $\alpha_{IV}$ we may also write

$$\left( \frac{dR}{dT} \right)_{IV} = \frac{G(2\alpha\phi + \beta(n + \phi - \dot{n}\phi))}{I^2 n (2+\beta)}. \tag{6}$$

We later use eqn 6 to confirm that the MTES is stably biased with negative $\beta$ values from IV measurements.

## 4 Measured RT derived from IV measurements

The standard procedure of IV measurements made over a range of bath temperatures was used assuming a thermal model of 4 giving $G = 20$ nW/K and $n = 3.73$ for the prototype MTES tested.

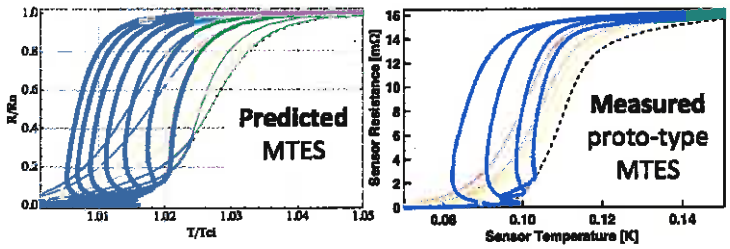


**Fig. 1** (Color online) $R$ vs. $T$ from IV measurements left predicted and right measured. Black dashed curve is for negligible self-field ($g \to 0$) and no applied field ($B_a = 0$), case 1 from reference[1]. Red to Violet curves are in order of increasing applied magnetic field $B_a$ from -2 to 10 $\mu$T. Thicker curves represent case 2 from[1] and the thin solid curves case 0 with a large negative self magnetic field.

With the known thermal parameters $G$ and $n$ the IV data collected at different $T_b$ are plotted in Fig. 1 on the right. These measurements are compared against the theoretical predicted MTES behavior shown on the left plot of Fig. 1 showing similar behavior as the applied magnetic field $B_a$ changes. We see that the yellow curve ($\beta_B > 0$, case 0) of Fig. 1 has an increased resistive transition width $\Delta T$ as compared to the black dashed curve ($\beta_B \approx 0$, case 1). With $g < 0$ as $B_a$ is increased you enter the curves where $\beta_B$ is negative, thick solid curves, ($\beta_B < 0$ case 2). As predicted a MTES can have its $\left(\frac{dR}{dT}\right)_{IV}$ (and the associated transition width $\Delta T$ either decrease or increase) by simply changing the applied magnetic field $B_a$. For the large $|g|$ limit we confirm that it is possible to make $\beta_B$ sufficiently negative such that the total $\beta = \beta_I + \beta_B$ is negative where the transition $RT$ projection's slope changes sign and the curve doubles back on itself as predicted.

By simply changing an applied magnetic field over an entire array of MTES sensors it is possible to change the width of the resistive transition *in situ*. Applications include tuning the applied field $B_a$ to an optimal value for a specific maximum photon energy for optimal energy resolution then changing the applied magnetic field $B_a$ to broaden the resistive transition over the array of MTESs and collect a spectrum over a larger spectral range without saturation.

In addition magnetic tuning can be used to change the shape of the resistive transition to improve the linearity of the detector response.

## 5 Negative $\beta$ Confirmation

- Negative $\left(\frac{dR}{dT}\right)_{IV}$ Argument.
  With the modest assumption that $G, \phi, I^2, n$ all $> 0$; then if our only additional assumption is $\alpha > 0$, it follows from Eq. 6 that $\left(\frac{dR}{dT}\right)_{IV} < 0$ implies $\beta < 0$. The measured thermal X-ray pulse signal direction implies the $\alpha > 0$ condition is satisfied therefore we have $\beta < 0$.
- Infinite $\left(\frac{dR}{dT}\right)_{IV}$ Argument.
  We see from measurements of IV curves at different bath temperatures for the data projected onto the $RT$-plane in Fig. 1 that there exists curves with

a region of $\left(\frac{dR}{dT}\right)_{IV} > 0$ that continuously transitions as $R/R_N$ is reduced to a region with $\left(\frac{dR}{dT}\right)_{IV} < 0$. In between these regions the slope is very sharp with $\left(\frac{dR}{dT}\right)_{IV} \to \infty$. By inspection of our equation 6 for $\left(\frac{dR}{dT}\right)_{IV}$ if $n$ and $I^2$ are both finite and $\neq 0$, then $\left(\frac{dR}{dT}\right)_{IV} \to \infty$ implies $\beta \to -2$. Our simulations show that the point where the the bias trajectory projected onto the $RT$-plane turns in the opposite direction and has infinite slope does correspond to $\beta = -2$.

## 6 Bias Stability Conditions

We reinvestigate the TES bias stability conditions to include the magnetic field dependence of the resistive transition. Additionally we wish to investigate what values of $\beta$ are allowed for stable operation, in particular are negative $\beta$ values stable, if so how negative can $\beta$ become and be stable and what constraints are imposed on other physical parameters.

The coupled nonlinear electrothermal differential equations describing a TES can be approximated by coupled linear differential equations for which analytic solutions exist. This system of coupled linear differential equations has solutions that are either over damped, under damped, or critically damped. Each type of solution can be either stable or unstable. In each of the three cases the stability condition is met if the real part of both eigenvalues $1/\tau_+$ and $1/\tau_-$ are positive ( $\mathrm{Re}[1/\tau_+] > 0 \wedge \mathrm{Re}[1/\tau_-] > 0$).

Using the variable definitions from the Irwin Hilton review article we find that the two eigenvalues agree but with the new definition of $\beta = \beta_I + \beta_B$, meaning adding the $\beta_B$ contribution.

The eigenvalues are simply $1/\tau_\pm = x \pm \sqrt{q}$, using the parameter definitions $x \equiv \frac{1}{2\tau_{el}} + \frac{1}{2\tau_I}$ and $q \equiv \frac{1}{4}\left(\left(\frac{1}{\tau_{el}} - \frac{1}{\tau_I}\right)^2 - 4\frac{R}{L_{ind}}\frac{\mathscr{L}(2+\beta)}{\tau}\right)$ with the natural time constant $\tau = C/G$ where $C$ is the heat capacity and $G$ is the thermal conductance between the sensor and the heat bath, $\tau_{el} = L_{ind}/(R_{sh} + R(1+\beta))$ is the electrical time constant with $L_{ind}$ the inductance connected in series with the TES and $R_{sh}$ the shunt resistor. $\tau_I = \tau/(1-\mathscr{L})$, with $\mathscr{L}$ the loop gain as defined in Irwin and Hilton satisfying $\mathscr{L} = \frac{\alpha P}{GT} = \frac{\alpha I^2 R}{GT}$.

- The conditions for stability:
  1. stable over damped$(q > 0) \wedge (x > \sqrt{q})$,
  2. stable under damped $(q < 0) \wedge (x > 0)$,
  3. stable critically damped $(q = 0) \wedge (x > 0)$.

The space of all stable bias operation is then given by

$$[(q > 0) \wedge (x > \sqrt{q})] \vee [(q \leq 0) \wedge (x > 0)]\,. \tag{7}$$

The derived set of inequalities for stability differ from the set of inequalities in the review article by Irwin and Hilton (equations 51, 52, and 53). We emphasize that the stability criteria up to this point are quite general and follows simply from the set of coupled linear differential equations describing the temperature $T(t)$ and current $I(t)$ time evolution of the TES.

Despite the complicated form for the stability space some simplifications exist. To reduce the complexity of the expressions, in what that follows we limit our discussion to the parameter space of greatest physical interest specific for TESs and consider $\mathscr{L} \geq 0$, which from the definition effectively assumes $\alpha \geq 0$. We also consider $\tau > 0$ and so too the resistances and inductances ($R$, $R_{sh}$, and $L_{ind}$).

Looking at solutions for the most negative $\beta$, stable bias with $\beta < -2$ exists but only for over damped solutions and also requires $\mathscr{L} < 1$ and $R < R_{sh}(\mathscr{L} - 1)/(1+\mathscr{L}+\beta)$, which implies that $R < R_{sh}$.

Assuming $\tau > 0 \wedge R_{sh} > 0 \wedge R > 0 \wedge L_{ind} > 0$ then no stable solution exists for $\beta \leq -2 \wedge (R \geq R_{sh} \vee \mathscr{L} \geq 1)$. This combined with the earlier statement means that $R < R_{sh}$ and $\mathscr{L} < 1$ is a necessary but not sufficient condition to stably bias with $\beta < -2$.

Stable critically damped solutions ($q = 0$) exist with $\beta = -2$, provided $\mathscr{L} < 1$, and $L_{ind} = \tau(R_{sh} - R)/(1 - \mathscr{L})$, which implies that $R < R_{sh}$.

For $R = R_{sh}$ and $\mathscr{L} = 1$ then if we define a variable $p \equiv 4L_{ind}/(R(2+\beta))$ we have stable under damped solutions for $\beta > -2 \wedge \tau < p$, stable over damped solutions for $\beta > -2 \wedge \tau > p$, and stable critically damped solutions for $\beta > -2 \wedge \tau = p$.

Stable critically damped solutions occur with $q = 0$, $\mathscr{L} > 1$, and $R > R_{sh}$ if and only if $\beta > -1 \wedge \frac{L_{ind}}{R(2+\beta)}\left(\mathscr{L} + 2\sqrt{\mathscr{L}} + 1\right) < \tau < \frac{L_{ind}}{R(1+\beta)^2}\left(2\sqrt{\mathscr{L}(2+\beta)(1+\mathscr{L}+\beta)} + 1 + \beta + \mathscr{L}(3+\beta)\right)$ or $-2 < \beta \leq -1 \wedge \tau > \frac{L_{ind}}{R(2+\beta)}\left(\mathscr{L} + 2\sqrt{\mathscr{L}} + 1\right)$.

## 7 Stability plots

The previous section we learned how exactly the TES or MTES tends to unstable solutions for larger $\mathscr{L}$, $L_{ind}$, or $R_{sh}$ ; or smaller $\tau$, $\beta$, or $R$. In figure 2 we present region plots of stability with device parameter values $C = 0.135$ pJ/K, $G = 20$ nW/K, $\tau = C/G = 675$ $\mu$s, $L_{ind} = 18$ nH, $R_{sh} = 0.2$ m$\Omega$ and $R_{sh} = 2.2$ m$\Omega$. We do not need to assume a specific $R_N$ value but plot $R$ to a typical value of the normal state resistance $R_N \approx 10$ m$\Omega$. Also in the figure are gray dashed lines going through $\beta = -2$ and $R = R_{sh}$ landmark values as a guide to the eye for comparisons. Different ranges are covered for the plots with axis $\log\mathscr{L}$ (left column) as compared to $\mathscr{L}$ (right column) plots of Fig 2.

An important result of our analysis is that stable operation in the underdamped regime is not insured with the condition $R > R_{sh}$. In contrast with equation (51) or Irwin and Hilton's review we find that for any $\beta$ and with $R > R_{sh}$ for sufficiently large $\mathscr{L}$ the device becomes unstable. In other words, there exists over damped solutions that pass the stability criteria of equation (51) but are unstable even for positive values of $\beta$ and $\mathscr{L}$. Our stability criteria for under damped operation also departs from equations (52) and (53) in the same article[6] when negative $\beta$ values are considered.

## References

1. J. E. Sadleir, S. J. Smith, S. R.Bandler, J. S.Adams, S. E.Busch, M. E. Eckart, J. A. Chevenak, R. L. Kelley, C. A. Kilbourne, F. S. Porter, J-P.Porst, J. R.

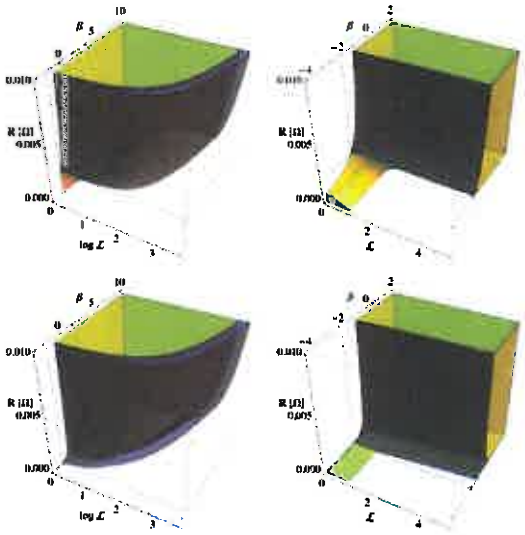

**Fig. 2** (Color online) Array of plots showing regions of bias stability with $L_{ind} = 18$ nH and $\tau = 675$ $\mu$s. Left and right columns plotting $\log\mathscr{L}$ and $\mathscr{L}$ respectively. Top and bottom rows have $R_{sh} = 2.2$ and 0.2 m$\Omega$ respectively. Purple/Yellow regions represent stable under damped and stable over damped respectively. Gray dashed lines are at $\beta = -2$ and $R = R_{sh}$.


Clem, IEEE Trans. App. SuperCond. **23**, 2101405 (2013).

2. J. E. Sadleir, S. J. Smith, S. R. Bandler, J. A. Chervenak, and J. R. Clem, Phys. Rev. Lett., **104**, 047003 (2010).
3. S. J. Smith et al J. App. Physics (accepted for publication).
4. J. E. Sadleir, PhD. Dissertation, University of Illinois Physics Dept. (2010).
5. J. E. Sadleir, S. J. Smith, Ian K. Robinson, F. M. Finkbeiner, J. A. Chervenak, S. R. Bandler, M. E. Eckart, and C. A. Kilbourne Phys. Rev. B, **84**, 184502 (2011).
6. K. D. Irwin and G. C. Hilton, in *Topics in Applied Physics: Cryogenic Particle Detection*, edited by C. Enss, (Springer, Berlin), (2005).
7. K. D. Irwin, Nuc. Inst. Meth. A **559**, 718 (2006).
8. A. Kozorezov, A. A. Golubov, D. D. E. Martin, P.A. Korte, M.A. Lindeman, R.A. Hijmering, J. van der Kuur, H. F. C. Hoevers, L. Gottardi, M.Y. Kupriyanov, J.K. Wigmore, Appl. Phys, Lett. **99** 063503 (2011).
9. A. Kozorezov, A. A. Golubov, D. D. E. Martin, P. A. J. de Korte, M. A. Lindeman, R. A. Hijmering, J.K. Wigmore, IEEE Trans. Appl. Supercond. **21** 250 (2011).
10. S.J. Smith, J.S. Adams, C.N. Bailey, S.R. Bandler, J.A. Chervenak, M.E. Eckart, F.M. Finkbeiner, R.L. Kelley, C.A. Kilbourne, F.S. Porter, J.E. Sadleir, J. Low Temp. Phys. **167** 168 (2012).